Supporting Information for Publication

Non-Viral In Vivo Delivery of CRISPR-Cas9 using Protein-Agnostic, High-Loading Porous Silicon and Polymer Nanoparticles

R. Brock Fletcher[1], Larry Stokes[1], Isom B Kelly III[1], Katelyn Henderson[1], Isabel Vallecillo-Viejo[1], Juan M. Colazo[1], Benjamin Wong[1], Fang Yu[1], Richard d'Arcy[1], Morgan Struthers[1], Brian C Evans[1], Jacob Ayers[1], Matthew Castanon[1], Michael J Weirich[1], Sarah Reilly[1], Shrusti Patel[1], Yoanna Ivanova[1], Carlos A. Silvera Batista[2], Sharon M. Weiss[3], Charles A. Gersbach[4], Jonathan Brunger[1], Craig L. Duvall*[,1]

[1] Dept. of Biomedical Engineering, Vanderbilt University, Nashville, TN, US 37235-1631
[2] Dept. of Chemical and Biomolecular Engineering, Vanderbilt University, Nashville, TN, US 37235-1631
[3] Dept. of Electrical Engineering, Vanderbilt University, Nashville, TN, US 37235-1631
[4] Dept. of Biomedical Engineering, Duke University, Durham, NC, US 27708
* Corresponding Author: craig.duvall@vanderbilt.edu

Contents

Supplementary Data....3
Figure S1 NanoSight Report Data....3
Figure S2 Quantification of Particle Porosity....4
Figure S3 Modeling of PSiNP pore Electrostatics....5
Figure S4 PSiNP Loading calculations and TGA measurements....6
Figure S5 Kinetics of BSA release from PSiNPs in PBS....7
Figure S6 Confirmation of optimal PEGDB coating of PSiNPs....8
Figure S7 Cas9 PSiNP dose response linear regression....9
Figure S8 IDAA indel quantification method....10
Figure S9 Editing in Ai9 mice following intramuscular administration of PSiNPs....11
Figure S10 Biodistribution measurements of PSINPs....12

Supplementary Data

Table S1- sgRNA Target Sequences

sgRNA Name	Purpose	Target Sequence (5’ to 3’)
sgAi9-L	Ai9 turn-on	AAAGAAUUGAUUUGAUACCG
sgAi9-R	Ai9 turn-on	GUAUGCUAUACGAAGUUAUU
Rosa26-L	Ai9 & mTmG cell line creation	GACUGGAGUUGCAGAUCACG
Rosa26-R	Ai9 & mTmG cell line creation	GAAGAUGGGCGGGAGUCUUC
MMP13-sg7272835	MMP13 knockout	UCGGAGCCUGUCAACUGUGG
sg-mTmG	mTmG turn-on	AUUAUACGAAGUUAUAUUAA

Table S2- Primer Sequences for IDAA and qPCR

Primer Name	Purpose	Sequence (5’ to 3’)
MMP13.FWD	qPCR	GGCCAGAACTTCCCAACCAT
MMP13.REV	qPCR	GAGCCCAGAATTTTCTCCCTCT
ActB.FWD	qPCR	GACTCATCGTACTCCTGCTTG
ActB.REV	qPCR	GATTACTGCTCTGGCTCCTAG
Rpl13a.FWD	qPCR	ATGTCCCCTCTACCCACAG
Rpl13a.REV	qPCR	TGAACCCAATAAAGACTGTTTGC
IDAA_Universal_FAM	IDAA	AGCTGACCGGCAGCAAAATTG
Ai9_1.FWD	IDAA	ttcggcttctggcgtgtg
IDAA_Ai9_2.FWD	IDAA	AGCTGACCGGCAGCAAAATTGcctctgctaaccatgttcatgcc
IDAA_Ai9_3.FWD	IDAA	AGCTGACCGGCAGCAAAATTGctgggcaacgtgctggttattg
IDAA_Ai9_4.REV	IDAA	AGCTGACCGGCAGCAAAATTGgtgtgaccggcggctctag
Ai9_5.REV	IDAA	cctcctcgcccttgctc

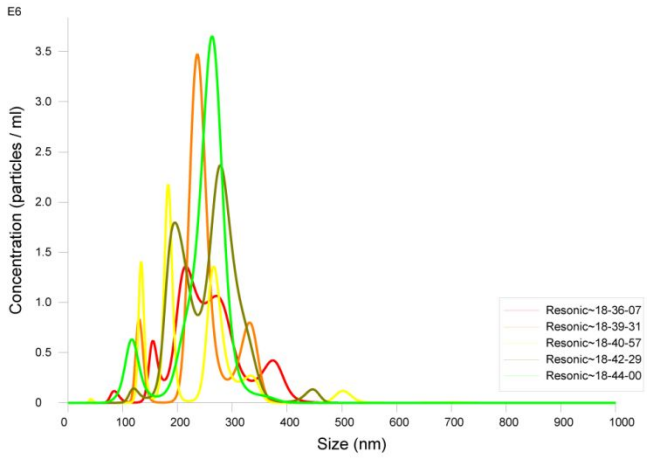

FTLA Concentration / Size graph for Experiment:

Capture Settings

Camera Type:	sCMOS
Laser Type:	Red
Camera Level:	2
Slider Shutter:	7
Slider Gain:	15
FPS	25.0
Number of Frames:	1498
Temperature:	20.4 - 20.6 ºC
Viscosity:	(Water) 0.985 - 0.991 cP
Dilution factor:	Dilution not recorded

Analysis Settings

Detect Threshold:	11
Blur Size:	Auto
Max Jump Distance:	Auto: 9.5 - 11.8 pix

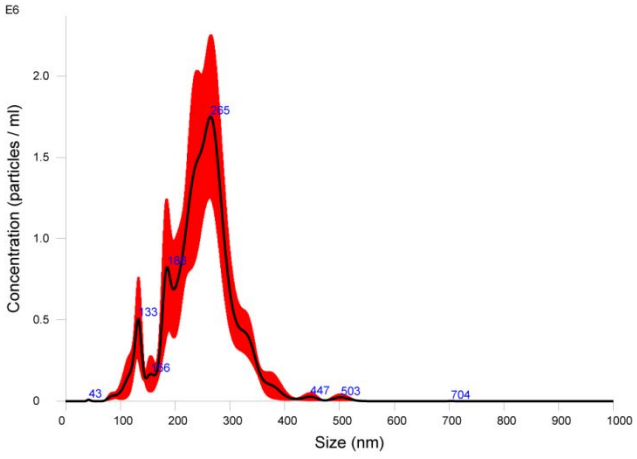

Averaged FTLA Concentration / Size for Experiment:
Error bars indicate + / -1 standard error of the mean

Results

Stats: Merged Data

Mean:	248.9 nm
Mode:	264.6 nm
SD:	59.8 nm
D10:	177.9 nm
D50:	251.4 nm
D90:	318.2 nm

Stats: Mean +/- Standard Error

Mean:	247.7 +/- 3.9 nm
Mode:	235.3 +/- 17.0 nm
SD:	60.7 +/- 6.0 nm
D10:	178.7 +/- 12.1 nm
D50:	250.6 +/- 4.0 nm
D90:	323.2 +/- 10.9 nm
Concentration (Upgrade):	1.92e+08 +/- 2.32e+07 particles/ml
	18.8 +/- 2.3 particles/frame
	25.2 +/- 2.9 centres/frame

Concentration measurements may require some caution due to noise
See summary file for more info

Figure S1 NanoSight Report Data

Raw NanoSight report data. Five independent measurements (graph on left) were performed and combined to make the graphic included in the main figure (graph on right). Additionally, statistics from the merged data (right graph) are boxed in green.

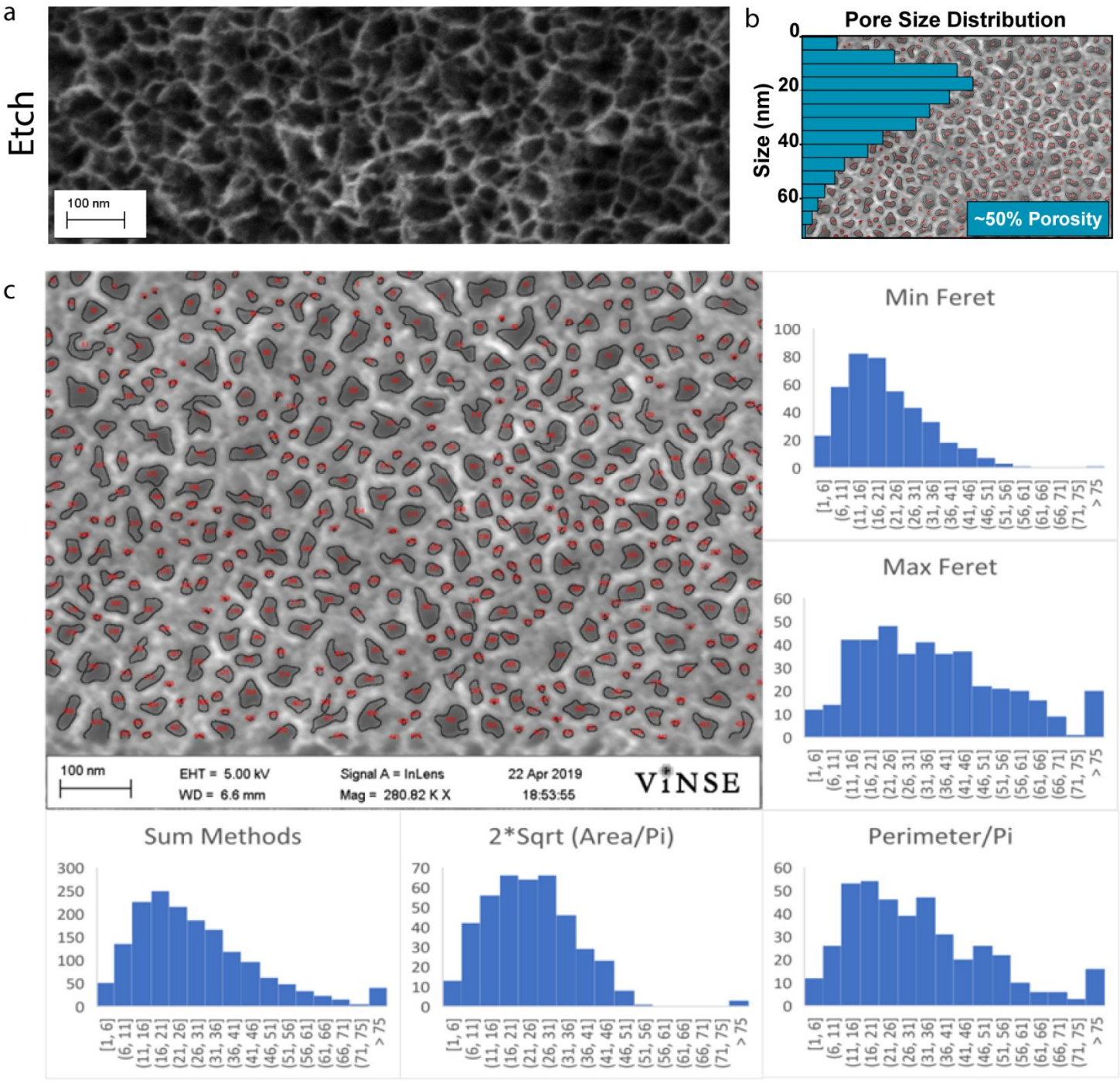

<u>Figure S2</u> Quantification of Particle Porosity

Center Image: Original inlay SEM image with overlay of ImageJ pore segmentation. Surrounding graphs are histograms of various pore size distribution quantification methodologies. Summing the different methods yields the “sum methods” plot, from which the main-manuscript figure was made.

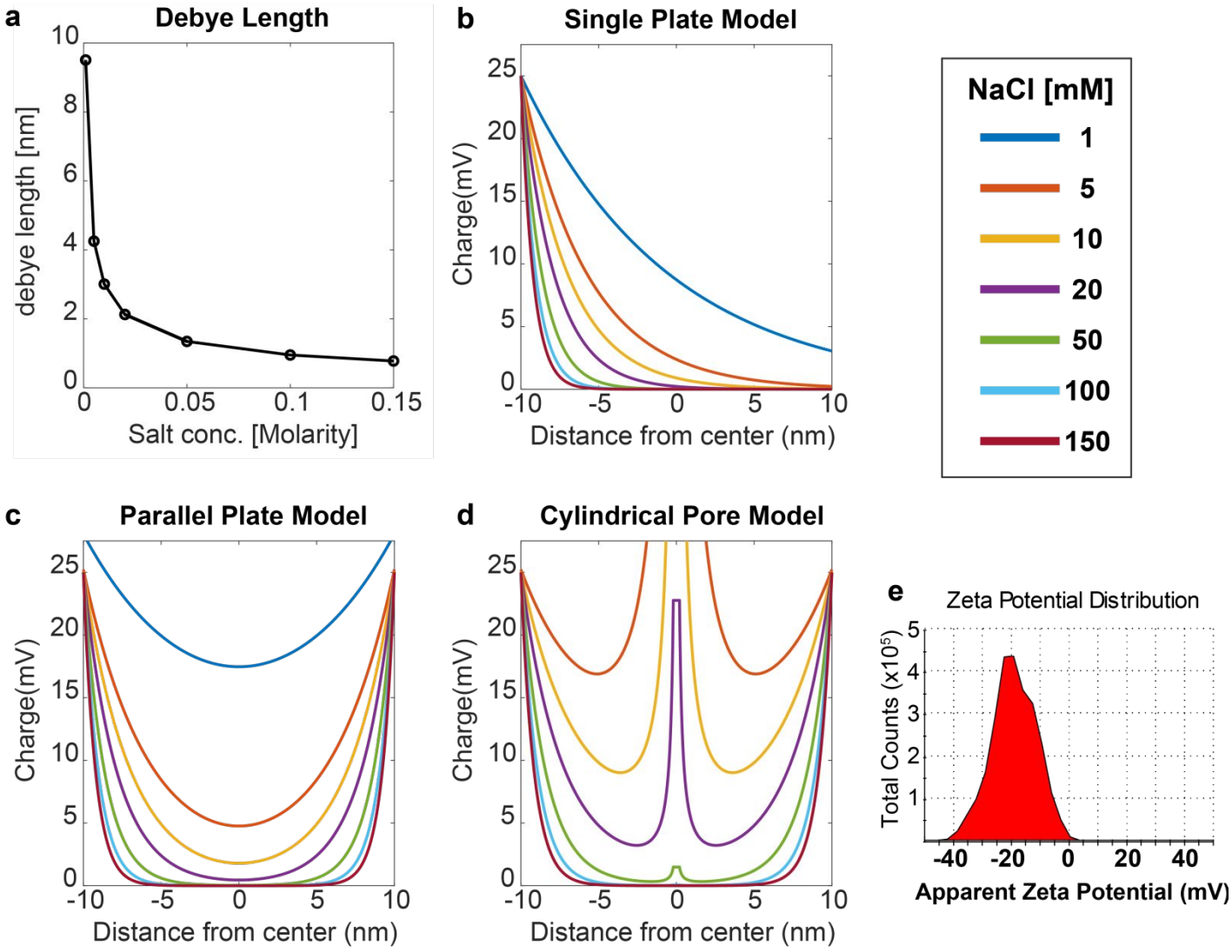

Figure S3 Modeling of PSiNP pore Electrostatics.
a) Debye Length as a function of NaCl concentration. (b) Electric field away from a single charged surface as a function of distance (x-axis) and NaCl concentration (line color). (c) Same as b but with two parallel plates 20 nm apart and using the linear superposition approximation. (d) Same as c but modeling within a cylinder instead. See github.com/BrockFletcher/Cas9_Silicon. (e) Zeta potential distribution measured of porous silicon nanoparticles graphed in **Error! Reference source not found.**b.

a

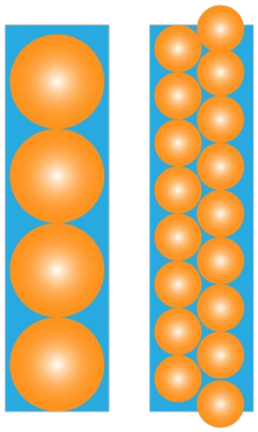

More Free Space

Less Free Space

Cylindrical Packing Factor

As Described by Mughal Et al, The maximum amount of volume small spheres can take up within a larger cylinder is dependent on the ratio of their radii. Considering proteins as spheres and the pores as cylinders, the theoretical values calculated here closely reflect the experimental results of protein loading.

b

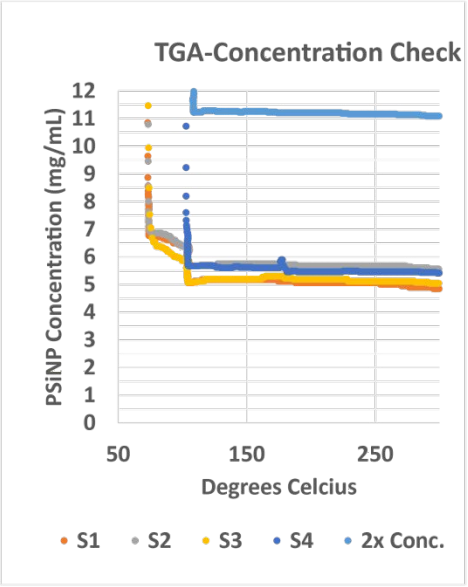

c

Constants			Vol% Si	Vol% Poly	Wt%
Protein Density	1.35		50	27	20
Silicon Density	2.49		37	20	15
Density Ratio:	1.84444		25	14	10
%Porosity	0.5		12	7	5
Pore Size (nm)	20		0	0	0

	BSA	Cas9 RNP	CRE	Cas9
Sphere Radius (nm)	3.3	10	3	9
Ratio	6.06	2.00	6.67	2.22
Packing Factor	0.6	0.475	0.6	0.525
Max Loading by Mass	= %Porosity * Packing Factor * (Protein Density/ Silicon Density)			
(Theory) Max Load by Mass	16.3%	12.9%	16.3%	14.2%
(Experi) Max Load by Mass	16.9	16.1	18.3	16.7

S1	S2	S3	S4	2xS
5.18	5.73	5.20	5.47	5.56
Mean	5.43	5.43		
StDev	0.21	0.11	SEM	
Mean /StDev	3.9%	2.0%	Mean /SEM	

Figure S4 PSiNP Loading calculations and TGA measurements.

a) Explanation of calculations and Packing factor. b) Thermogravimetric analysis used to accurately determine PSiNP Concentration. c) Estimations of maximal cargo loading into porous silicon nanoparticles.

a

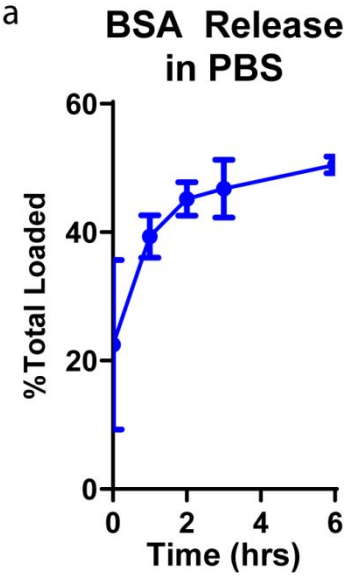

<u>Figure S5</u> Kinetics of BSA release from PSiNPs in PBS.
a) Bovine Serum Albumin release kinetics from PSiNPs in infinite sink of PBS over 6 hours.

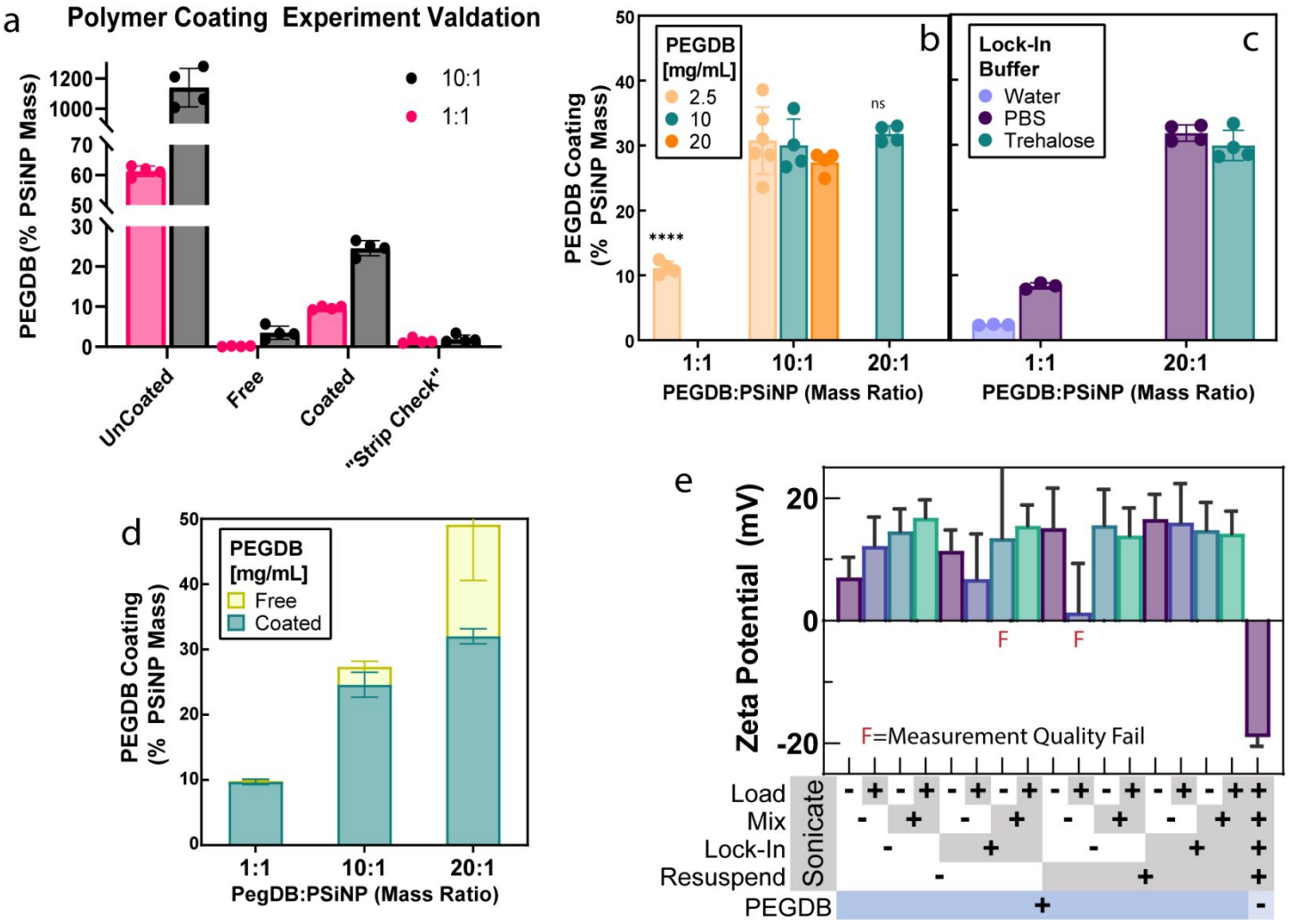

<u>Figure S6</u> Confirmation of optimal PEGDB coating of PSiNPs

a) Quantification of labeled PEGDB at each step of the polymer coating assay. The protocol is detailed in the methods section, but, briefly, “Uncoated” refers to the PEGDB which does not coat the PSiNPs and thus does not pellet. “Free” refers to PEGDB which comes off in an added centrifugal wash step. “Coated” refers to PEGDB which was stably coating the porous silicon nanoparticles. “Strip Check” is a validation of the methods, as we use a stripping buffer to remove the PEGDB from the PSiNPs to measure concentration, and this is an additional step to ensure all PEGDB polymer has been removed from the PSiNPs. b) Effects of PEGDB concentration and PEGDB:PSiNP ratio on coating. c) Water vs. PBS and trehalose vs. PBS effects on PEGDB coating. Trehalose was not tested in the 1:1 group because we had not yet hypothesized its potential benefit. Water was not tested in the 20:1 group because it had already been proven inferior in the prior 1:1 testing. d) Amount of uncoated PEGDB as a function of incubation ratio. e) Zeta potential measurements corresponding to sonication-DLS measurements in Figure 3.

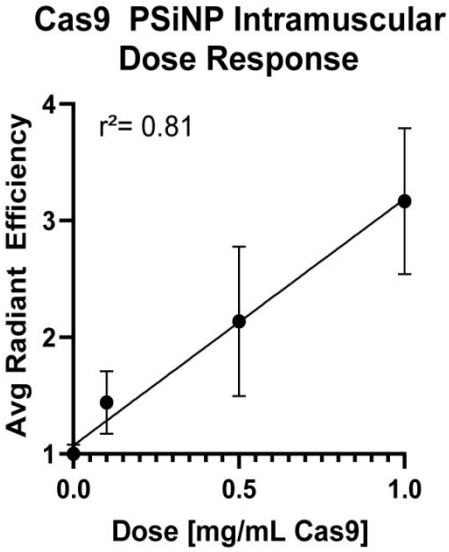

Figure S7 Cas9 PSiNP dose response linear regression

Dose response of IVIS signal from injected tibialis anterior muscle of Ai9 mice, plotted as the injected concentration (in mg/mL of Cas9 protein, 20 µL injection) vs average radiant efficiency normalized to negative control (Buffer only).

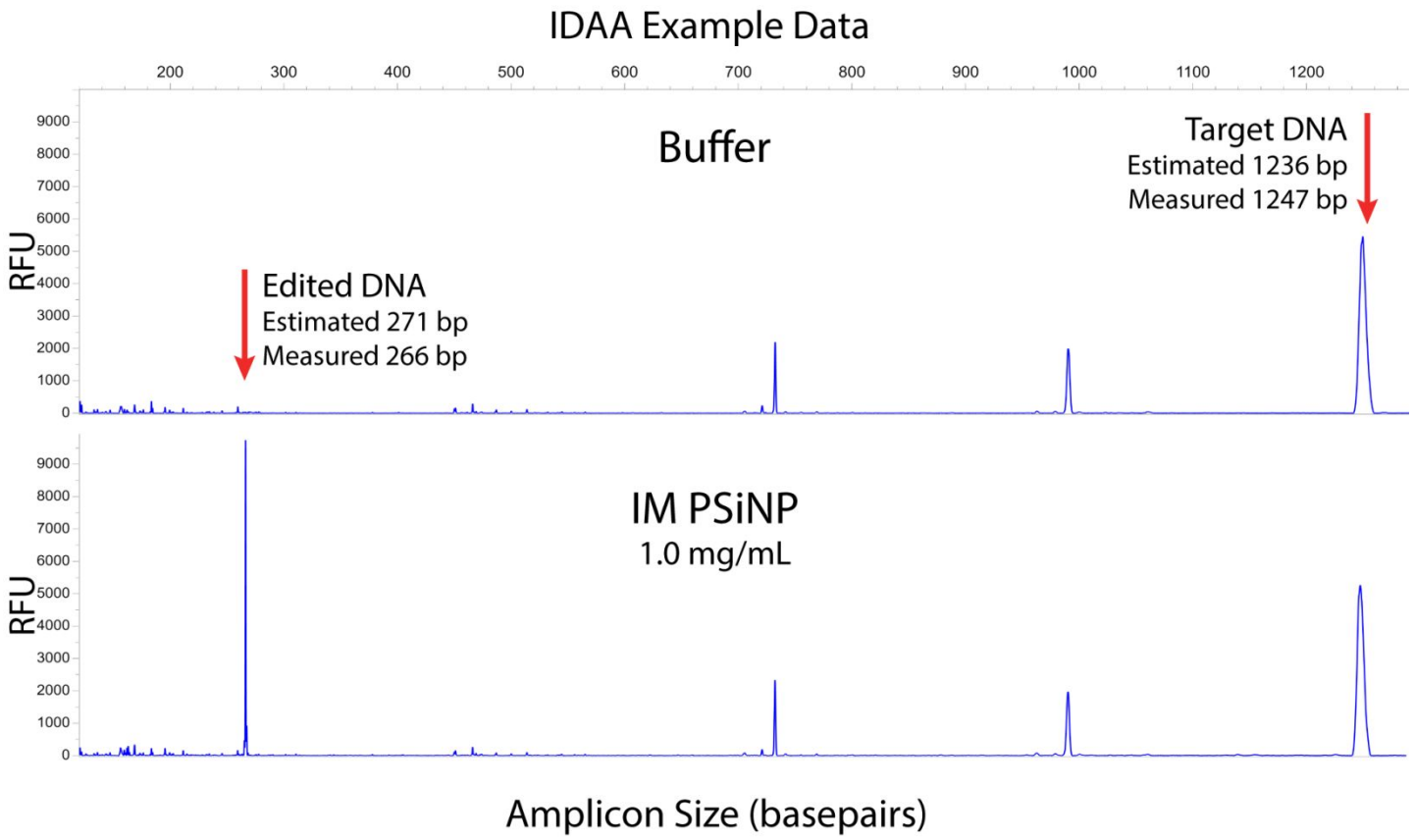

<u>Figure S8</u> IDAA indel quantification method

a) Example fragment analysis traces used to quantify deletion the deletion strategy used in indel detection by amplicon analysis. Note the increase in signal at ~271 bp, the expected size of the Ai9 amplicon after deletion of nearly 1000 bp.

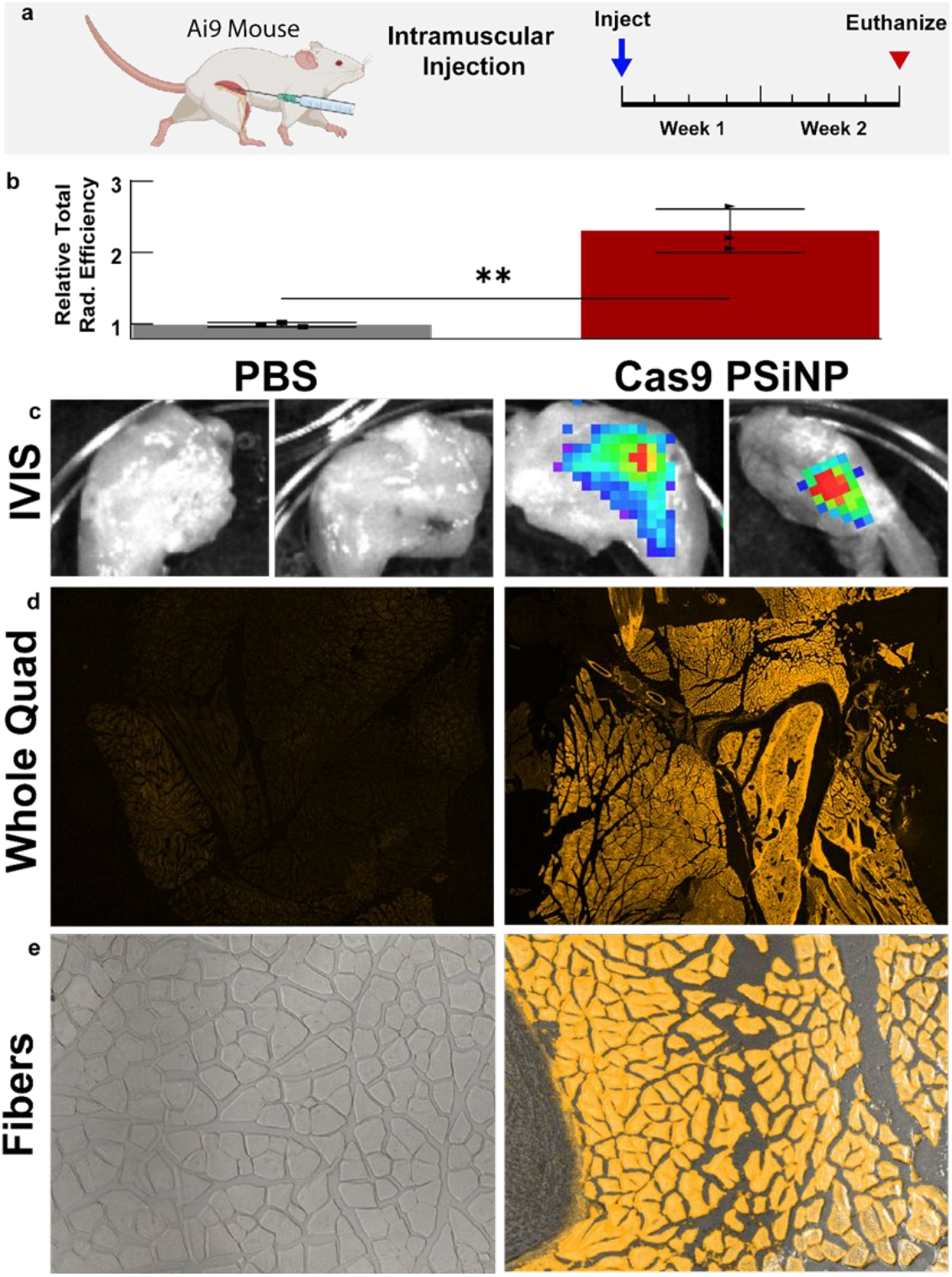

<u>Figure S9</u> Editing in Ai9 mice following intramuscular administration of PSiNPs.
(a) Experimental timeline for direct quadriceps injection study. Muscle was injected with PSNPs or PBS and harvested two weeks after the second injection. (b) IVIS (total radiant efficiency) data from mouse muscle after sacrifice. (c) Representative IVIS images of legs from each group. (d) Cryohistology to visualize tdTomato fluorescence in edited muscle fibers. (e) High magnification of muscle group to visualize edited fibers.

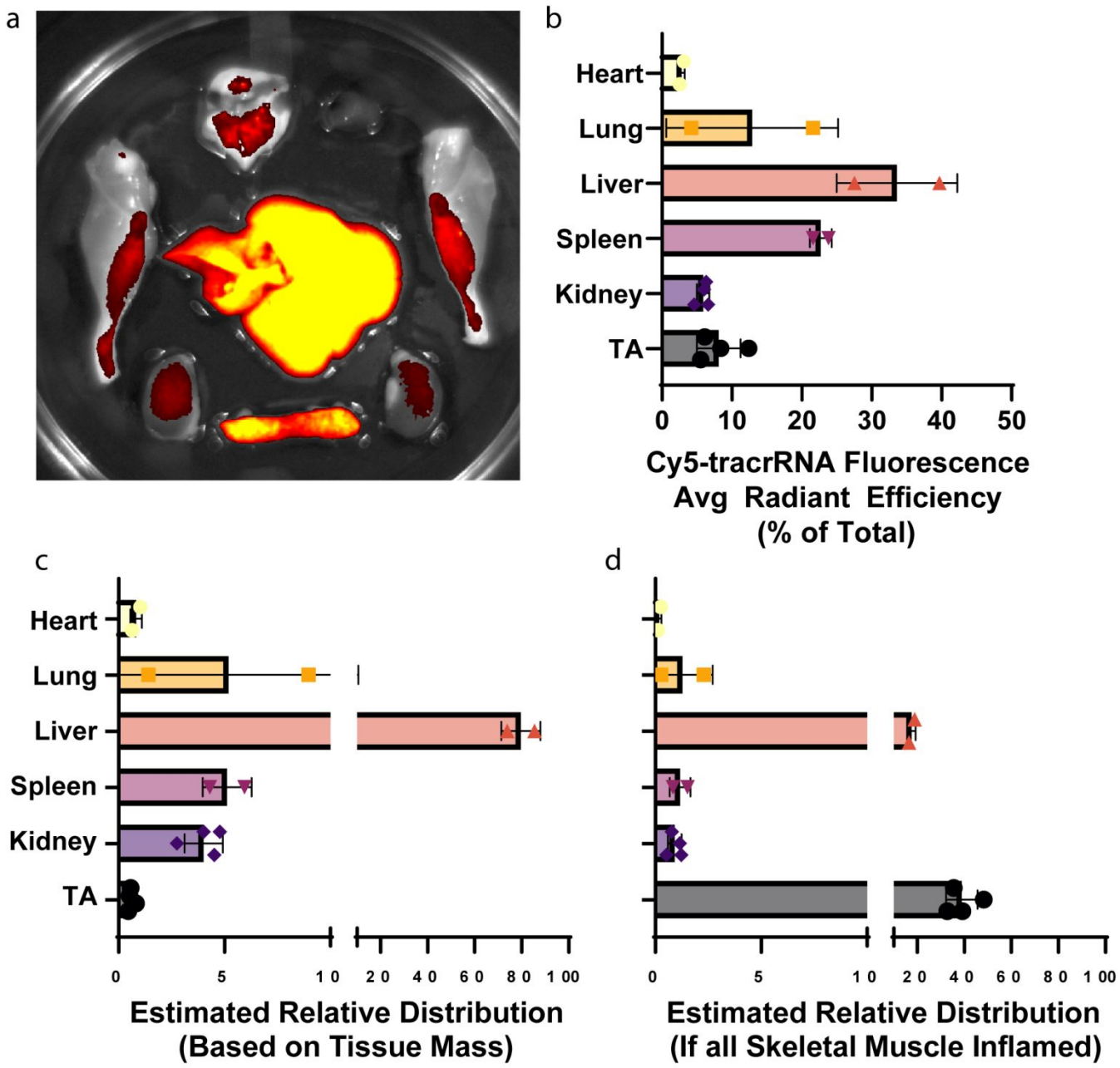

Figure S10 Biodistribution measurements of PSINPs.
(a) Example image displaying biodistribution of Cy5-labeled Cas9 RNP using IVIS Imaging (b) Quantification of IVIS imaging. The average radiant efficiency of each reason was summed up, and data is presented as a percentage of the total by organ. (c) Multiplying average radiant efficiency over background of the tissue by the measured mass of the tissue yields an estimated biodistribution in each organ (percent injected dose). (d) Repeating the estimation used in section c but multiplying by the total muscle mass yields the relative biodistribution if all skeletal muscle was inflamed like the tibialis anterior.